Drug Design, Development and Therapy

Dovepress
Taylor & Francis Group

Open Access Full Text Article

ORIGINAL RESEARCH

Irisin Mitigates Doxorubicin-Induced Cardiotoxicity by Reducing Oxidative Stress and Inflammation via Modulation of the PERK-eIF2α-ATF4 Pathway

Zilong Zhang*, Xiaolin Yu*, Jie Li, Xin Shen, Wenbo Fu, Yongguo Liu, Xiangyu Dong, Zhao Wang

Department of Cardiology, Cardiac and Pan - Vascular Medicine Center, People's Hospital of Xinjiang Uygur Autonomous Region, Xinjiang, People's Republic of China

*These authors contributed equally to this work

Correspondence: Zilong Zhang; Zhao Wang, Department of Cardiology, Cardiac and Pan - Vascular Medicine Center, People's Hospital of Xinjiang Uygur Autonomous Region, No. 91 Tianchi Road, Urumuqi, Xinjiang, 830001, People's Republic of China, Tel +86 8560287, Email zhangzilong871203@163.com; xjzzqwz@163.com

Purpose: Doxorubicin (DOX), an anthracycline antibiotic, has limited clinical use due to its pronounced cardiotoxicity. Irisin, a myokine known for its metabolic regulation, has shown therapeutic effects on cardiovascular disease. This study investigates the potential cardioprotective function of irisin in reducing the cardiac injury induced by DOX.

Methods: In vitro, H9c2 cells were pretreated with irisin (20 nM) for 24 hours before exposure to DOX (1 μM). In vivo, C57BL/6 mice were administered DOX (5 mg/kg/week, i.p.) for 4 weeks, reaching a cumulative dose of 20 mg/kg. Irisin (1 mg/kg/ 3 days, i.p.) was administered to the mice both 7 days prior to and during DOX injection.

Cardiac function was evaluated by echocardiography, and cardiac histology was assessed using HE, WGA, and Masson staining. Myocardial injury markers were quantified using ELISA, and apoptosis was analyzed via TUNEL staining. Oxidative stress was determined by measuring antioxidase activity, MDA and GSH levels, and DHE staining, while mitochondrial superoxide production was assessed using MitoSOX Red. Mitochondrial morphology and function evaluated using transmission electron microscopy and Seahorse analysis, respectively Inflammatory cytokines were quantified in serum and cell supernatants. The role of the PERK-eIF2α-ATF4 pathway mediated by irisin was investigated by Western blot. Using adeno-associated virus serotype-9 carrying mouse FNDC5 shRNA (AAV9-shFNDC5) further validated the protective role of irisin in DOX-induced myocardial injury.

Results: Irisin reduced DOX-induced cardiac dysfunction and fibrosis. Moreover, irisin mitigated oxidative stress and inflammation through inhibiting the PERK-eIF2α-ATF4 pathway activated by DOX, thus preserving mitochondrial function. While cardiac FNDC5 knockdown exacerbated DOX-induced heart injury and PERK-eIF2α-ATF4 activation, which was partially reversed by irisin.

Conclusion: Irisin mitigates oxidative stress and inflammation by modulating the PERK-eIF2α-ATF4 pathway, highlighting its potential as a prospective approach for combating DOX-induced cardiotoxicity.

Keywords: irisin, doxorubicin, cardiac injury, PERK-eIF2α-ATF4

Introduction

Doxorubicin (DOX), a potent anthracycline, is widely used to treat a variety of cancers due to its broad-spectrum efficacy.[1–3] However, the dose-dependent cardiotoxicity associated with DOX has become increasingly prominent.[3–5] Prolonged administration of DOX can lead to irreversible cardiomyopathy and eventually result in heart failure, with potentially fatal outcomes.[3,6] This highlights the urgent need for effective therapies to alleviate DOX-induced cardiotoxicity.

The heart, as a highly energy-demanding organ, is rich in mitochondria that provide the majority of energy for cardiomyocytes.[7,8] DOX-induced cardiotoxicity is primarily mediated by the overproduction of reactive oxygen species (ROS), which disrupt the mitochondrial respiratory chain, leading to oxidative stress.[1,9] Oxidative stress damages lipids, proteins, and DNA, which compromises the integrity and function of cellular membranes, triggering extensive cardiomyocyte apoptosis.[5]

Received: 16 September 2024
Accepted: 24 January 2025
Published: 15 February 2025

Furthermore, DOX activates the inflammatory response by upregulating interleukin-1β (IL-1β) and tumor necrosis factor-α (TNF-α) levels.[5,10,11] Meanwhile, accumulating lipid peroxides induced by DOX cause aseptic inflammatory responses, further exacerbating oxidative damage and leading to an amplified cascade of inflammation and oxidative stress.[11–13] Thus, suppressing DOX-induced oxidative stress and inflammation may be a potential strategy to mitigate DOX-induced cardiotoxicity.

The production of secreted or membrane-bound proteins, as well as calcium homeostasis, lipid biosynthesis, and protein folding, depends on the endoplasmic reticulum (ER).[14,15] Inflammation, ischemia, and excess protein synthesis are examples of stress signals that set off the ER stress,[16,17] executed by protein kinase R (PKR)-like ER kinase (PERK), activating transcription factor 6α (ATF6α), and inositol-requiring enzyme 1 alpha (IRE1α), collectively known as the unfolded protein response (UPR).[15,18] Noticeably, PERK and the downstream signaling, eukaryotic translation initiation factor 2α (eIF2α), and activating transcription factor 4 (ATF4) is crucial for eliminating misfolded proteins via lysosomal degradation.[10,19] And the prolonged activation can lead to cell apoptosis via CCAAT-enhancer-binding protein homologous protein (CHOP) and caspases.[20] Recent studies have linked sustained activation of the PERK-eIF2α-ATF4 pathway to heart failure and diabetic cardiomyopathy,[12,21,22] but its role in DOX-induced heart injury remains poorly understood.

Irisin, a bioactive peptide generated during exercise, is cleaved from fibronectin type III domain-containing protein 5 (FNDC5).[23,24] Traditionally, irisin has been recognized for its role in promoting the browning of white adipose tissue, thereby enhancing thermogenesis, which underscores its beneficial impact on metabolic diseases.[24,25] Recent studies suggest that irisin also offers benefits in ischemic and pressure-overload heart diseases by preserving mitochondrial function and reducing oxidative damage.[26,27] Considering these findings, we hypothesized that irisin might protect against DOX-induced cardiotoxicity through modulation of the PERK-eIF2α-ATF4 pathway.

Materials and Methods

Reagents

Recombinant irisin (#HY-P72534) and doxorubicin (DOX, #HY-15142) were obtained from Medchemexpress Co., Ltd. (MCE, US). MDA (#S0131S), SOD (#S0101S), GSH (#S0053), NADPH (#S0179), and ATP content (#S0026) assay kits were obtained from Beyotime Biotechnology (Shanghai, China). The irisin assay kit (#EK-067-29) was obtained from Phoenix Pharmaceuticals (Burlingame, CA, USA).

Animals

This study received approval from the Ethics Committee of the People's Hospital of Xinjiang Uygur Autonomous Region (#2021-02-08) in accordance with the NIH Guide for Care and Use of Laboratory Animals. Male C57BL/6 mice (7–8 weeks old) were provided by Gempharmatech Co., Ltd. (Nanjing, Jiangsu, China) and maintained under specific pathogen-free conditions with a 12-hour light/dark cycle at 22°C. After a one-week acclimation period, the mice were randomly assigned to three groups: control, DOX-treated (DOX), and DOX plus irisin-treated (DOX+irisin). DOX or vehicle (5 mg/kg/week, i.p.) was administered for 4 weeks, reaching a cumulative dose of 20 mg/kg.[9,28] Following established protocols with some modifications, recombinant irisin (1 mg/kg/3 days, i.p.) was administered for 7 days prior to and during DOX treatment.[27,28]

To specifically reduce cardiac irisin levels, mice were intravenously injected with FNDC5 shRNA (AAV9-cTnT-shFNDC5) or a negative control (AAV9-cTnT-shNC) (Genechem Co., Ltd., China) at a concentration of 1×10^{11} viral genomes. 4 weeks after the viral injection, mice were treated according to the methods before. Primer sequences used for shFNDC5 are listed:

CCCTCTGTGAACATCATCAAACTCGAGTTTGATGATGTTCACAGAGGG. Echocardiography was conducted 7 days after the final dose of DOX treatment, followed by euthanasia with an overdose of tribromoethanol for serum and tissue collection. The experimental design is outlined in Figures 1A and 6A.

Cell Culture and Viability

H9c2 rat cardiomyocytes purchased from Cell Bank of the Chinese Academy of Sciences (Shanghai, China) were grown in Dulbecco's Modified Eagle Medium (DMEM) supplemented with 10% fetal bovine serum (FBS), 100 mg/mL

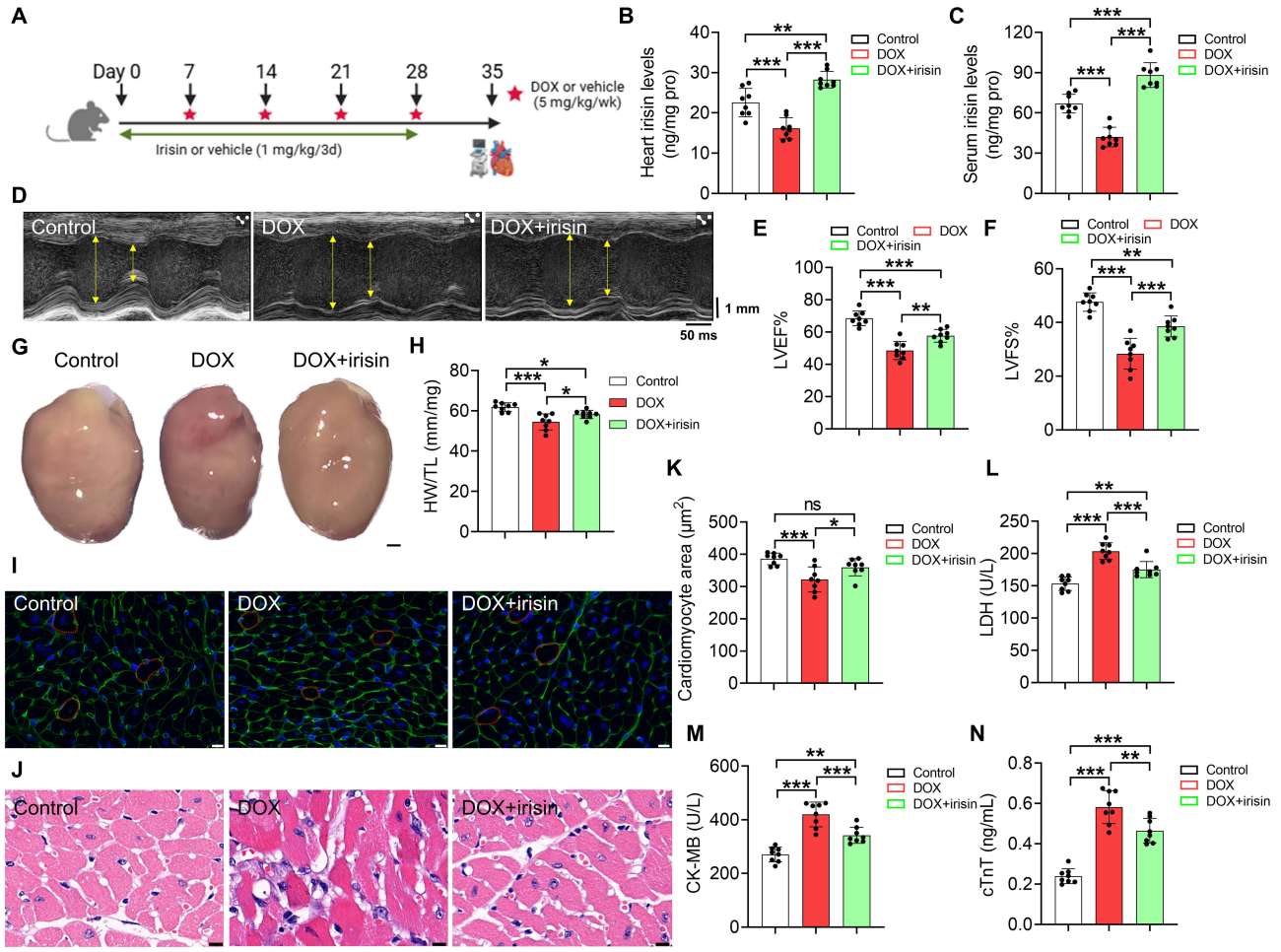

Figure 1 Irisin mitigated DOX-induced cardiac dysfunction and myocardial injury (n = 8 per group). (**A**) Schematic flowchart of irisin treatment and the construction of the DOX-induced cardiotoxicity in mice. (**B** and **C**) Heart irisin level (**B**) and serum irisin level (**C**). (**D**) Representative echocardiography images of heart in M-mode. (**E** and **F**). Quantification of LVEF% (**E**) and LVFS% (**F**). (**G**) Representative hearts gross morphology images, scale bar= 2 mm. (**H**) The heart weight to tibia length (HW/TL). (**I–K**) Representative hearts sections of WGA staining (**I**) and HE staining (**J**) and the qualification of cardiomyocyte area (**K**), scale bar= 10 μm. (**L–N**). LDH (**L**), CK-MB (**M**), and cTnT (**N**) contents in the serum. Data are expressed as mean ± SD. * P < 0.05, **P < 0.01, and ***P < 0.001 was considered statistically significant and ns indicates not significant.

streptomycin, and 100 U/mL penicillin, and maintained at 37°C in a humidified incubator with 5% CO_2. Cell viability was evaluated using the CCK-8 assay (Dojindo Molecular Technologies, Kyushu, Japan) in H9c2 cells cultured in 96-well plates and treated with different concentrations of DOX (0.5 μM, 1 μM, 2 μM, 4 μM) for 24 h. After a 2-h incubation with CCK-8 solution at 37°C, absorbance was measured at 450 nm. To investigate irisin's protective effects against DOX-induced toxicity, H9c2 cells were pretreated with varying concentrations of irisin (5 nM, 10 nM, 20 nM, 30 nM, 40 nM) for 24 h, followed by an additional 24-h DOX exposure. Based on these results and previous studies,[29,30] 20 nM irisin and 1 μM DOX were selected for subsequent experiments.

Echocardiography

Mice placed on a heated imaging platform were anesthetized with 2% isoflurane for cardiac function assessment detected by the Vevo 2100 Imaging System (Visual Sonics, Toronto, Canada) with a 30 MHz transducer. A blinded investigator performed echocardiographic measurements at the mid- ventricular level.

Histological Analysis

Heart tissues were fixed in 4% formalin for 24 h, dehydrated, and embedded in paraffin. Sections of 5 μm thickness were prepared and stained with hematoxylin and eosin (HE) for general histology. Fibrosis was evaluated using Masson's

https://doi.org/10.2147/DDDT.S492691

trichrome staining on paraffin-embedded sections. For wheat germ agglutinin (WGA) staining, the fixed sections were incubated with WGA (5 μg/mL) for 10 min and then stained with DAPI. All slides were captured under a light microscope (Nikon H550L, Tokyo, Japan) blindly. Collagen area and cardiomyocyte area was quantified using ImageJ software.

Detection of Myocardial Injury Markers

Cardiac-specific troponin T (cTnT), lactate dehydrogenase (LDH), and creatine kinase isoenzymes (CK-MB) levels in the serum were quantified using ELISA assay kits for CK-MB (#8671), LDH (#12239), and cTnT (#13150) from Meimian Industrial Co., Ltd. (Nanjing, Jiangsu, China).

Oxidative Stress Detection

For hearty tissue, superoxide dismutase (SOD) activity, malondialdehyde (MDA) levels, glutathione (GSH) content, and nicotinamide adenine dinucleotide phosphate (NADPH) levels were measured using the assay kits according to the instructions.

TUNEL Staining

Heart sections were fixed, embedded in paraffin, and sliced into 5 μm sections. After deparaffinization, rehydration, and permeabilization with 0.1% Triton X-100, the sections were washed with PBS and incubated with the TUNEL apoptosis detection kit (#C1091, Beyotime). Apoptotic cells (TUNEL-positive) were observed using a fluorescence microscope (Olympus IX83, Tokyo, Japan).

Dihydroethidium (DHE) Staining

Heart tissues were embedded in OCT, cryosectioned to 10 μm thickness, and incubated with 5 μM DHE at 37°C for 30 min in the dark. Following PBS washes, fluorescence was visualized under a fluorescence microscope.

Transmission Electron Microscopy

Cardiac tissues were fixed in 2.5% glutaraldehyde, post-fixed with 1% osmium tetroxide, dehydrated, and embedded in epoxy resin. Ultrathin sections (70 nm) were cut, placed on copper grids, and stained with uranyl acetate and lead citrate. Images were acquired using a transmission electron microscope (JEM-1400PLUS, JEOL, Japan) at 80 kV to evaluate mitochondrial structure, myofibril arrangement, and cellular integrity. Pathologists performed these assessments blindly.

LDH Release

The LDH level in cell culture supernatants was measured using the LDH assay kit (#ab65393) from Abcam Inc. (Boston, MA, USA), in accordance with the instructions. Absorbance at 492 nm was recorded using a microplate reader.

Mitochondrial Superoxide Production

H9c2 cells were incubated with 3 μM MitoSOX^{TM} Red (#M36007) from Thermo Fisher (Waltham, MA, US) at 37°C for 15 min. Images were visualized using a fluorescence microscope.

Mitochondrial Oxygen Consumption Rate (OCR)

As previously described, aerobic respiration of H9c2 cells was measured using the Seahorse XF24 analyzer (Agilent Technologies, Santa Clara, CA).[31] Briefly, cells were seeded overnight in 24-well plates and then incubated at 37°C in Seahorse assay media (pH 7.4) containing 2 mm glutamine, 1 mm pyruvate, and 1 g/L D-glucose in a non-CO_2 incubator. Baseline measurements were obtained after sequentially adding oligomycin A (4 μM, MCE), FCCP (3 μM, MCE), and rotenone/antimycin A (1 μM each, Sigma) at 37°C. Oxygen consumption rates were normalized to cell number (pmol O_2 /min/10^4 cells).

Mitochondria were isolated from heart tissues following standard protocols[32] and then resuspended in mitochondrial assay solution (MAS, pH 7.2) containing 70 mm sucrose, 220 mm mannitol, 10 mm KH_2PO_4, 5 mm $MgCl_2$, 2 mm

HEPES, 1 mm EGTA, and 0.2% fatty acid-free BSA. Mitochondria (5 μg/well) were cultured in MAS supplemented with 10 mm pyruvate, 2 mm malate, and 5 mm ADP on Cell-Tak-coated Seahorse XF24 plates (22.4 μg/mL). After a 30-min incubation at 37°C, oxygen consumption rates (OCR) were recorded following the addition of oligomycin A (5 μM), FCCP (5 μM), and a rotenone/antimycin A mix (10 μM/2 μM) and normalized to protein content.

ATP Content Detection

Cardiac ATP levels were measured using commercial assay kit (#S0027, Beyotime). Briefly, heart tissues were homogenized using ATP lysis buffer and centrifuged to collect supernatants. The supernatant was measured at 560 nm to quantify ATP content based on a standard curve.

Inflammatory Factor

Inflammatory cytokines content in the serum and supernatant were measured by the Elisa assay kits including IL-1β (#MLB00C), IL-6 (#M6000B), and TNF-α (#MTA00B) obtained from R&D Systems (Minneapolis, MN, USA) in accordance with the instructions.

Western Blots

Proteins were isolated from heart tissue using RIPA lysis buffer with a protease inhibitor cocktail. The lysate was centrifuged at 13,000g for 30 min at 4°C. Soluble proteins in the supernatant were separated by SDS-PAGE and transferred onto PVDF membranes. After blocking with 5% non-fat milk, the membranes were incubated overnight at 4°C with primary antibodies (Table 1), followed by incubated with secondary antibodies conjugated with HRP at room temperature for 2 h. Immunoreactive signals were detected, and band intensities were quantified using ImageJ software.

Quantitative Polymerase Chain Reaction (qPCR)

Total RNA was extracted from cardiac tissues using TRIzol. Reverse transcription was performed with the PrimeScript RT Reagent Kit (#RR036B, TaKaRa, Otsu, Japan), and gene quantification was detected using Bio-Rad's SYBR Green (Hercules, CA, USA). Gene expression was analyzed using the $2^{\Delta\Delta Ct}$ method, with GAPDH as the normalization control. Primers used in the study from TSINGKE Biosystems (Beijing, China) are listed in Table 2.

Statistical Analysis

Statistical analysis was performed using GraphPad Prism v.8.0 (La Jolla, CA, USA). The Shapiro–Wilk test was used to assess normality. Data are expressed as mean ± standard deviation (SD). For two-group comparisons, paired or unpaired two-tailed Student's t-tests were used, while for multiple groups, one-way ANOVA followed by Tukey's multiple

Table 1 Primary Antibodies for Western Blot

Name	Catalog	Species	Dilutions	Vendor
Bax	60267-1-Ig	Mouse	1:5000	Proteintech
Bcl2	26593-1-AP	Rabbit	1:1000	Proteintech
α-SMA	14395-1-AP	Rabbit	1:2000	Invitrogen
Collagen Type I	67288-1-Ig	Mouse	1:5000	Proteintech
TGF-β	ab215715	Rabbit	1:1000	Abcam
Phospho-PERK (Thr980)	MA5-15033	Rabbit	1:1000	Invitrogen
PERK	3192	Rabbit	1:1000	CST
Phospho-eIF2α (Ser51)	9721	Rabbit	1:1000	CST
eIF2α	9722	Rabbit	1:1000	CST
ATF4	11815	Rabbit	1:1000	Abcam
CHOP	15204-1-AP	Rabbit	1:1000	Proteintech
β-actin	66009-1-Ig	Mouse	1:20000	Proteintech

https://doi.org/10.2147/DDDT.S492691

Table 2 Primer Sequences

Gene	Species	Sequences 5′-3′
IL-1β	Mouse	F: TGGGCCTCAAAGGAAAGAAT
		R: CAGGCTTGTGCTCTGCTTGT
TNF-α	Mouse	F: ACCCTCACACTCAGATCATCTTC
		R: TGGTGGTTTGCTACGACGT
Fndc5	Mouse	F: ATGAAGGAGATGGGGAGGAA
		R: GCGGCAGAAGAGAGCTATAACA
Fndc5	Rat	F: CAGCAGAAGAAGGATGTGAG
		R: GGCAGAAGAGAGCTATGACA
GADPH	Rat	F: GACATGCCGCCTGGAGAAAC
		R: AGCCCAGGATGCCCTTTAGT
GAPDH	Mouse	F: GTATGACTCCACTCACGGCAAA
		R: GGTCTCGCTCCTGGAAGATG

comparisons test was applied. *P < 0.05, **P < 0.01, and ***P < 0.001 was considered statistically significant and ns indicates not significant.

Results

Irisin Mitigated DOX-Induced Cardiac Dysfunction and Myocardial Injury

Firstly, we grouped C57BL/6J mice as depicted in Figure 1A. Compared to controls, reduced serum and myocardial irisin levels were observed in DOX-treated mice, indicating that irisin expression may adaptively change in response to DOX administration (Figure 1B–D). Meanwhile, DOX-treated mice showed decreased left ventricular ejection fraction (LVEF %) and left ventricular fractional shortening (LVFS%) detected by the echocardiography (Figure 1D and F). However, irisin markedly improved the cardiac function impaired by DOX (Figure 1D and F).

Moreover, DOX resulted in cardiac atrophy as shown in Figure 1G and H, which was restored by irisin treatment (Figure 1G and H). Histological changes of cardiomyocytes determined by HE and WGA staining also demonstrated that irisin improved structure disruption caused by DOX treatment (Figure 1I–K). Surged LDH, CK-MB, and cTnT levels in the serum further supported cardiotoxicity induced by DOX. As expected, we observed that irisin impede the increase in serum myocardial injury markers triggered by DOX (Figure 1L–N). Collectively, these data suggest that irisin attenuated DOX-induced cardiotoxicity and improved mice cardiac function.

Irisin Alleviated Myocardial Fibrosis and Apoptosis Caused by DOX

Previous findings have indicated that DOX induces structural disruptions in cardiomyocytes, ultimately leading to impaired cardiac function.[28,33,34] As shown in Figure 2A, HE staining revealed significant damage to myocardial structures in the DOX group, characterized by disorganized and loosely arranged cardiomyocytes, along with inflammatory cell infiltration. Masson trichrome staining further indicated that DOX treatment led to cardiac fibrosis and collagen deposition (Figure 2A and B). Notably, irisin treatment effectively mitigated the structural damage and inhibited the myocardial fibrosis induced by DOX (Figure 2A and B). This anti-fibrotic effect of irisin was further validated by the inhibited levels of fibrosis-related proteins, including Col1α1, α-SMA, and TGF-β (Figure 2C).

Additionally, TUNEL staining of mouse heart sections showed that irisin reduced DOX-induced apoptosis, reflected by a decrease in TUNEL-positive cells (Figure 2D–E). Caspase-3, a key marker of apoptotic activity, was significantly activated in the hearts following DOX stimulation but was suppressed by irisin treatment (Figure 2F). Furthermore, irisin upregulated the anti-apoptotic gene Bcl-2 and downregulated the pro-apoptotic gene Bax compared to the DOX-treated mice (Figure 2G). These findings collectively suggest that irisin effectively alleviated DOX-induced cardiac fibrosis and cardiomyocyte apoptosis.

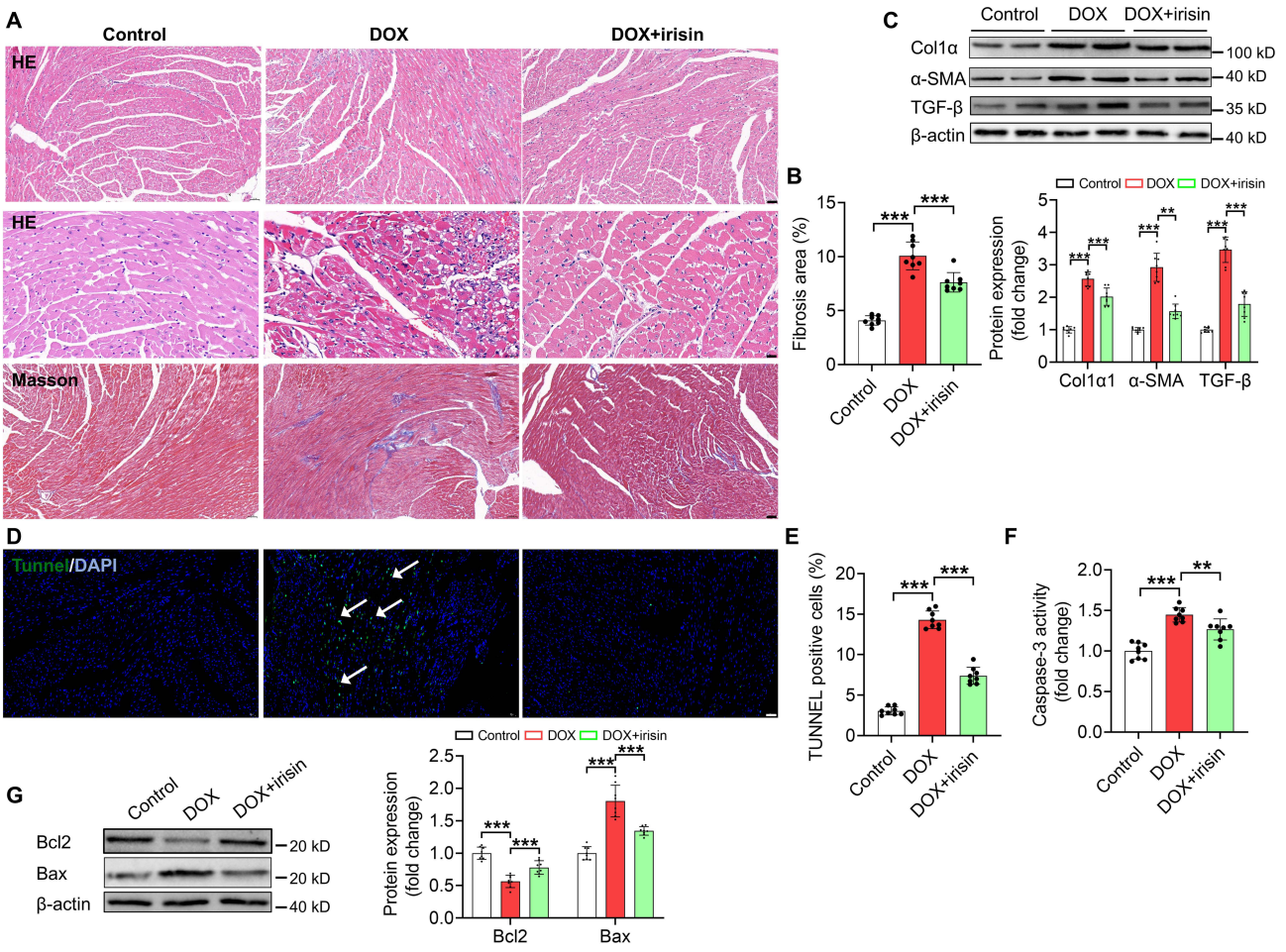

Figure 2 Irisin alleviated DOX-induced myocardial fibrosis and apoptosis (n = 8 per group). (**A**). Representative heart sections stained with HE (upper, scale bar=50 μm; mid, scale bar =20 μm) and Masson trichrome (below, scale bar=50 μm). (**B**). Quantification of the fibrosis area of the heart sections. (**C**). Representative immunoblots (top) and the quantification (bottom) for Col1α1, α-SMA, and TGF-β expression in heart tissues. β-actin as a loading control. (**D**) Representative heart sections stained with DAPI (blue) and TUNEL assay kit (green), scale bar=50 μm, arrows point to TUNEL positive cells. (**E**) Quantification of the TUNEL positive cells of the heart sections. (**F**) Caspase-3 activity of heart tissues. (**G**) Representative immunoblots and the quantification for Bcl-2 and Bax expression in heart tissues. β-actin as a loading control. Data are expressed as mean ± SD. **P < 0.01, and ***P < 0.001 was considered statistically significant.

Irisin Attenuates Myocardial Oxidative Stress and Inflammation in DOX Mice

Oxidative damage is recognized as a primary cause of DOX-induced cardiotoxicity, leading to cardiomyocyte apoptosis and contributing to the development of cardiac dysfunction.[1,5,35] DOX administration resulted in an increased fluorescence intensity in DHE-stained cardiac tissue, which was reduced by irisin treatment (Figure 3A). Furthermore, we evaluated the levels of MDA (a byproduct of lipid peroxidation), SOD activity, NADPH oxidase activity (a key intracellular antioxidant), and GSH (another intracellular antioxidant) in the heart. Our results indicated that irisin suppressed the elevated levels of MDA, GSH, and NADPH while preserving SOD activity compared to the DOX group (Figure 3B–E).

Increasing evidence indicates that inflammation is another critical factor in DOX-induced myocardial injury.[4,36] DOX directly activates inflammatory pathways, creating a storm of inflammatory factors that, together with oxidative stress, induces myocardial apoptosis.[37,38] Here, we found increased IL-1β and TNF-α levels in the serum of the DOX group, which were mitigated by irisin treatment (Figure 3F and G). In addition, DOX upregulated the mRNA levels of these pro-inflammatory cytokines, which were markedly downregulated in the irisin treated heart (Figure 3H–J). These findings collectively suggest that irisin alleviates DOX-induced cardiotoxicity by inhibiting oxidative stress and inflammatory responses.

https://doi.org/10.2147/DDDT.S492691

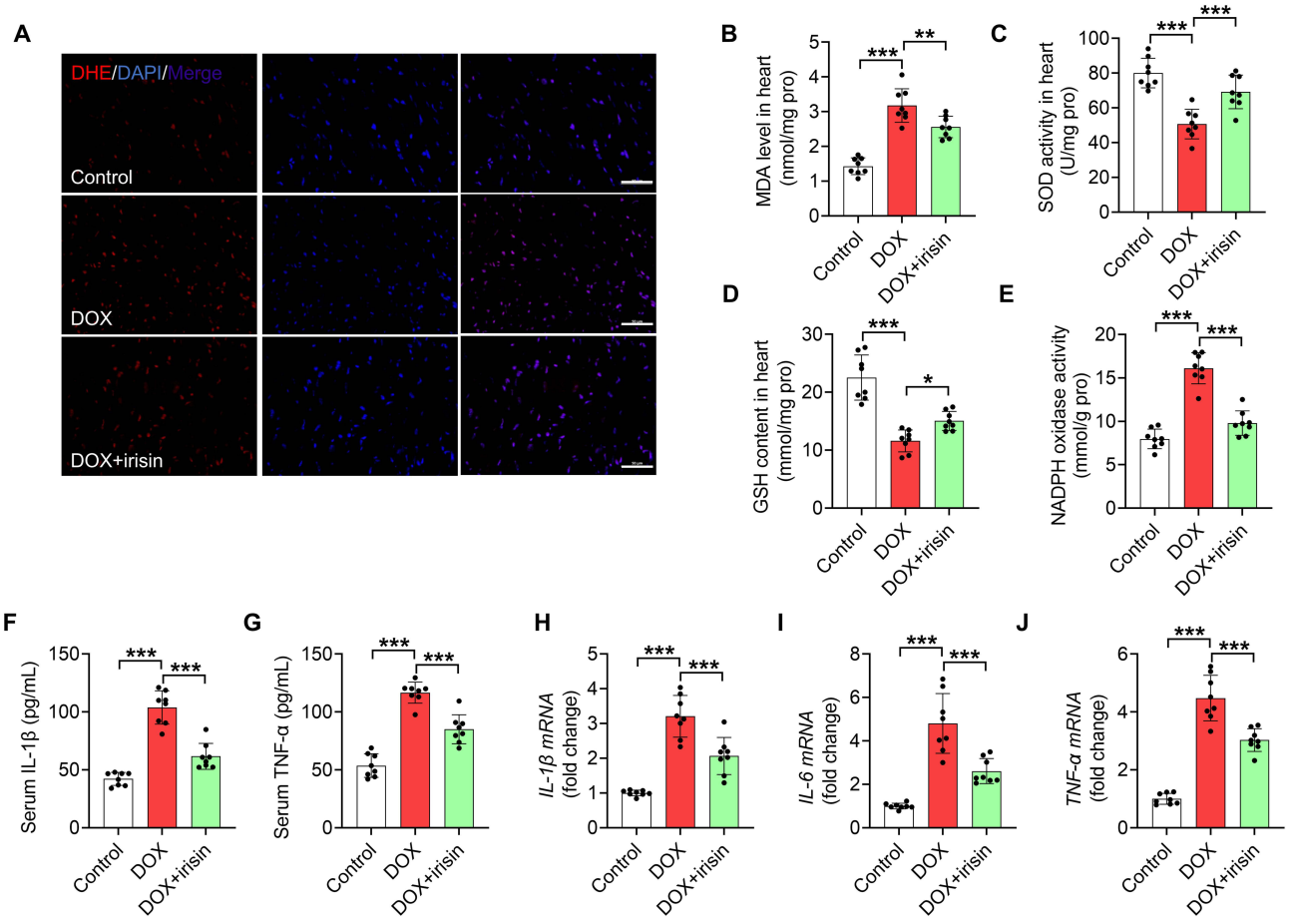

Figure 3 Irisin alleviated DOX-induced myocardial inflammation and oxidative stress (n = 8 per group). (**A**) Representative dihydroethidium (DHE) staining of heart sections, scale bar=50 μm. (**B–E**). MDA levels (**B**), SOD activity (**C**), NADPH activity (**D**), and GSH (**E**) content in heart tissues. (**F** and **G**). IL-1β (**F**) and TNF-α levels (**G**) in serum. (**H–J**). mRNA levels of IL-1β (**H**), IL-6 (**I**), and TNF-α (**J**) in heart tissues. Data are expressed as mean ± SD. * P < 0.05, **P < 0.01, and ***P < 0.001 was considered statistically significant.

Irisin Improved Mitochondrial Function and Attenuated ER Stress Signaling in Cardiac Injury Induced by DOX

Excessive ROS production triggered by DOX directly results in myocardial impaired mitochondrial function.[39,40] Transmission electron microscopy revealed that mitochondria from heart of the DOX-treated group were disorganized, swollen, and exhibited loss of cristae (Figure 4A). In contrast, irisin treatment significantly improved the mitochondrial ultrastructure (Figure 4A). Mitochondria are the primary organelles responsible for energy production, while abnormal mitochondrial morphology is typically associated with impaired respiratory function.[3,41] Seahorse analysis demonstrated that irisin effectively restored myocardial mitochondrial respiration, which was inhibited by DOX (Figure 4B–D). Additionally, ATP content measurements indicated that irisin could partially recover the energy production in myocardial tissue that was impaired by DOX (Figure 4E).

Under stress conditions, large amounts of misfolded proteins in the ER triggers the UPR, which is crucial for maintaining redox homeostasis.[16,18] While transient activation of the UPR is important for reducing protein load and maintaining ER homeostasis, excessive ER stress activation can lead to energy depletion, mitochondrial damage, and apoptosis.[14,17] Prior research has suggested that irisin modulates ER-mitochondrial interactions and ameliorates myocardial ischemia/reperfusion injury.[27] While transient activation of the UPR is important for reducing protein accumulation and maintaining ER homeostasis, excessive ER stress activation can lead to energy depletion, mitochondrial damage, and apoptosis.[15,18] Here, we manifested that the expression levels of p-PERK, p-eIF2α, ATF4, and the downstream gene CHOP were elevated following DOX treatment compared to controls. However, irisin treatment significantly

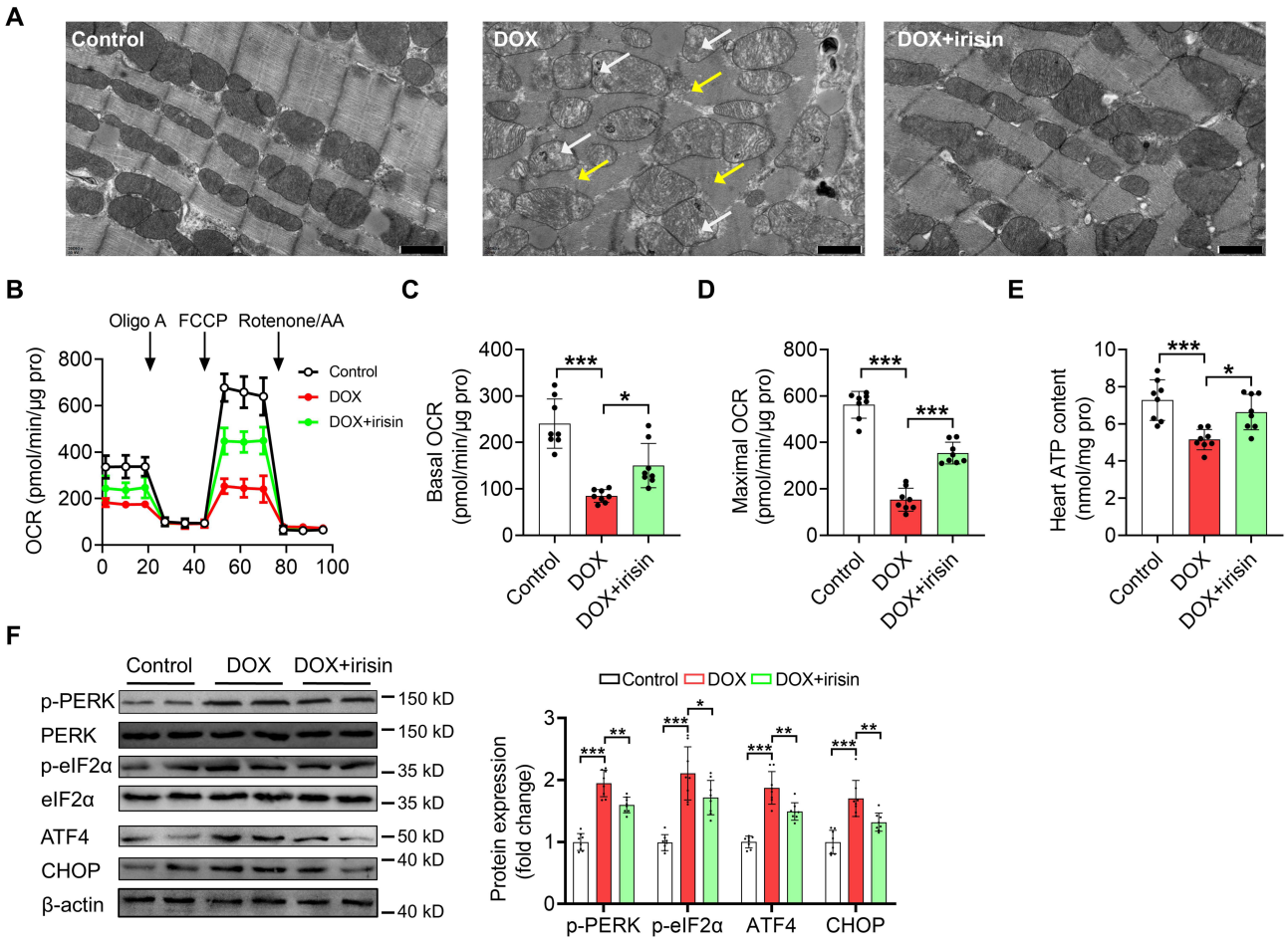

Figure 4 Irisin improved the mitochondrial function and inhibited ER stress in heart toxicity induced by DOX (n = 8 per group). (**A**) Representative ultrastructural images of the ventricular myocardium in mice. Yellow arrows point to fragmentation of muscle bands and white arrows point to abnormal shape of mitochondria, scale bar=1 μm. (**B**) Isolated mitochondria OCR from the hearts in the presence of pyruvate and malate. (**C** and **D**) Qualification of the basal OCR (**C**) and FCCP-stimulated maximal OCR (**D**). (**E**) ATP content in heart tissues. (**F**) Representative immunoblots and the quantification for protein expression of phospho- and total PERK, phospho-eIF2α, total-eIF2α, ATF4, and CHOP in heart tissues. β-actin as a loading control. Data are expressed as mean ± SD. * P < 0.05, **P < 0.01, and ***P < 0.001 was considered statistically significant.

downregulated these signaling pathways (Figure 4F). These findings collectively demonstrate that irisin effectively ameliorates mitochondrial function and suppresses ER stress in heart toxicity induced by DOX.

Irisin Alleviated DOX-Induced H9c2 Cell Injury and Mitochondrial Homeostasis Disruption

For further investigating the role of irisin on cardiomyocytes under DOX-induced stress in vitro, rat myocardial H9c2 cells were cultured with varying concentrations of DOX, resulting in significant decreased cell viability (Figure 5A). Pretreatment with irisin at concentrations of 20, 30, and 40 nM showed a protective effect on cardiomyocyte viability without exhibiting cytotoxicity following DOX exposure (Figure 5B), consistent with previous findings.[30,42] Based on these results, 1 μM DOX and 20 nM irisin were selected for subsequent experiments. DOX-treated H9c2 cells showed increased lactate dehydrogenase (LDH) levels in the culture medium (Figure 5C). In agreement with the in vivo results, irisin significantly enhanced mitochondrial respiration, including both basal and maximal OCR, which had been impaired by DOX treatment (Figure 5D). Additionally, DOX exposure led to an increase in IL-1β, IL-6, and TNF-α levels, in the supernatant (Figure 5E–G). DOX also induced a marked increase in intracellular ROS generation, as indicated by the enhanced MitoSOX™ Red fluorescence (Figure 5H). Notably, irisin suppressed inflammatory responses and inhibited mitochondrial ROS production in DOX-treated H9c2 cells (Figure 5A–H). These findings further suggest that irisin

https://doi.org/10.2147/DDDT.S492691

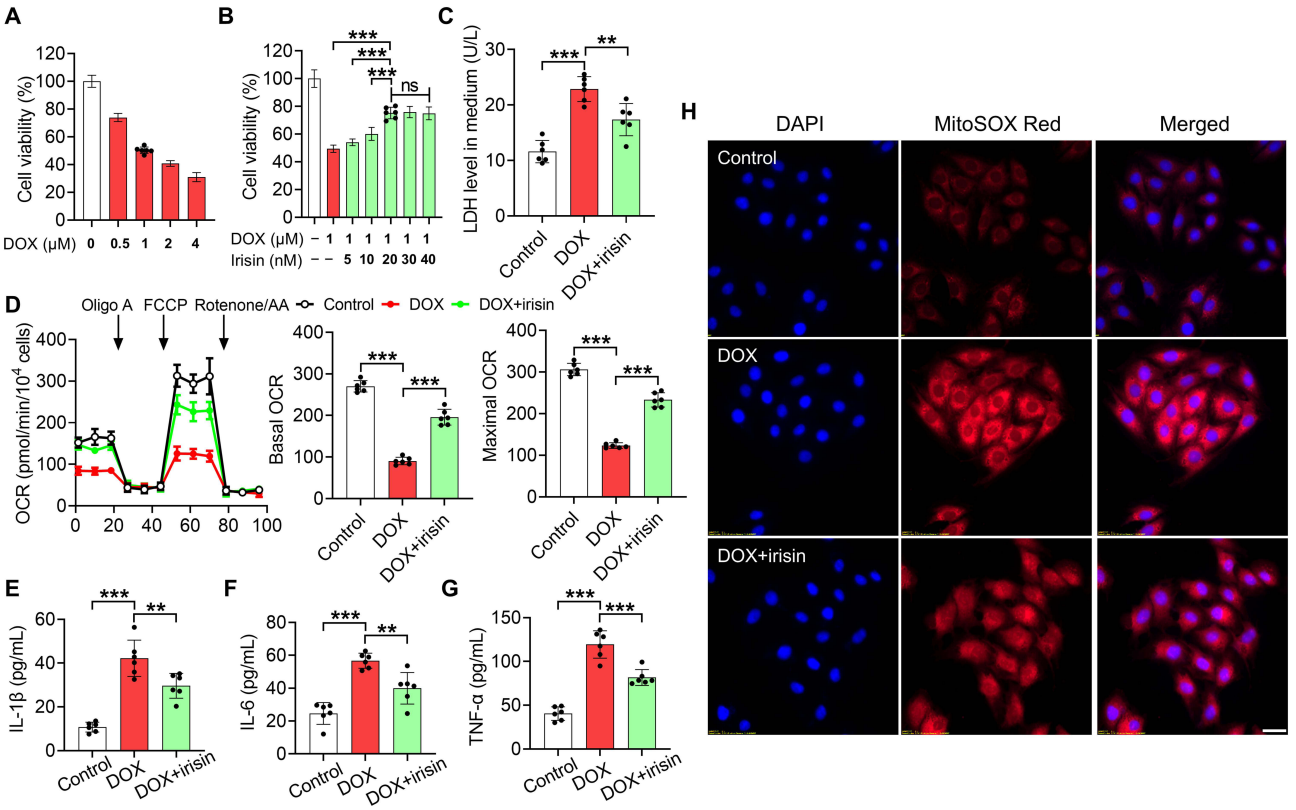

Figure 5 Irisin alleviated DOX-induced H9c2 cell injury and mitochondrial homeostasis disruption (n = 6 per group). (**A**) Cell viability of H9c2 exposure to DOX for 24 h. (**B**) Cell viability of H9c2 pretreatment with irisin for 24 h with or without 1 μM DOX for 24 h. (**C**) LDH level in the culture medium. (**D**) OCR curve (left) and qualification of the basal respiration (middle) and maximum respiration (right) of H9c2 cells. (**E–G**) IL-1β (**E**), IL-6 (**F**), and TNF-α (**G**) levels in the supernatants. (**H**) Representative fluorescence images of H9c2 cells stained with MitoSOX™ Red, scale bar=10 μm. Data are expressed as mean ± SD. **P < 0.01, and ***P < 0.001 was considered statistically significant and ns indicates not significant.

exerts protective effects on mitochondrial function, and reduces inflammation and oxidative stress in DOX-induced cardiomyocyte injury.

Irisin Protects Against DOX-Induced Myocardial Injury Through Regulating the PERK-eIF2α-ATF4 Pathway

To date, we have demonstrated that exogenous irisin exerts protective effects against DOX-induced myocardial injury, aligning with findings from previous studies.[27,28] Next, we sought to explore the role of endogenous irisin and the underlying mechanisms involved in DOX-induced cardiotoxicity. Initially, decreased FNDC5 mRNA expression was observed in both heart tissues and H9c2 cells following DOX stimulation (Figure S1A and S1B), which help explain the reduced cardiac irisin levels seen in Figure 1B.

To investigate whether endogenous irisin has a protective effect against the progression of DOX-induced cardiomyopathy, we selectively downregulated FNDC5 expression in the mouse heart using a single injection of AAV9 carrying FNDC5 shRNA (Figure 6A and Figure S2A). As shown in Figure S2B, AAV9-shFNDC5 effectively knocked down FNDC5 mRNA in the heart, causing reduced irisin levels both in heart tissues and serum (Figure S2C and S2D). Meanwhile, FNDC5 deficiency resulted in persistently reduced irisin levels in both the heart and serum following DOX injection (Figure 6B and C). Under normal conditions, mice among groups showed no differences in cardiac function and body weight (Figure S2E–H). However, mice injected with AAV9-shFNDC5 exhibited exacerbated cardiac dysfunction after DOX treatment, as evidenced by decreased LVEF% and LVFS% compared to the DOX+shNC group (Figure 6D–F). Interestingly, exogenous irisin replenishment improved the cardiac dysfunction caused by FNDC5 knockdown under DOX stress, accompanied by increased heart and serum irisin contents (Figure 6B–F). Moreover, the DOX-induced

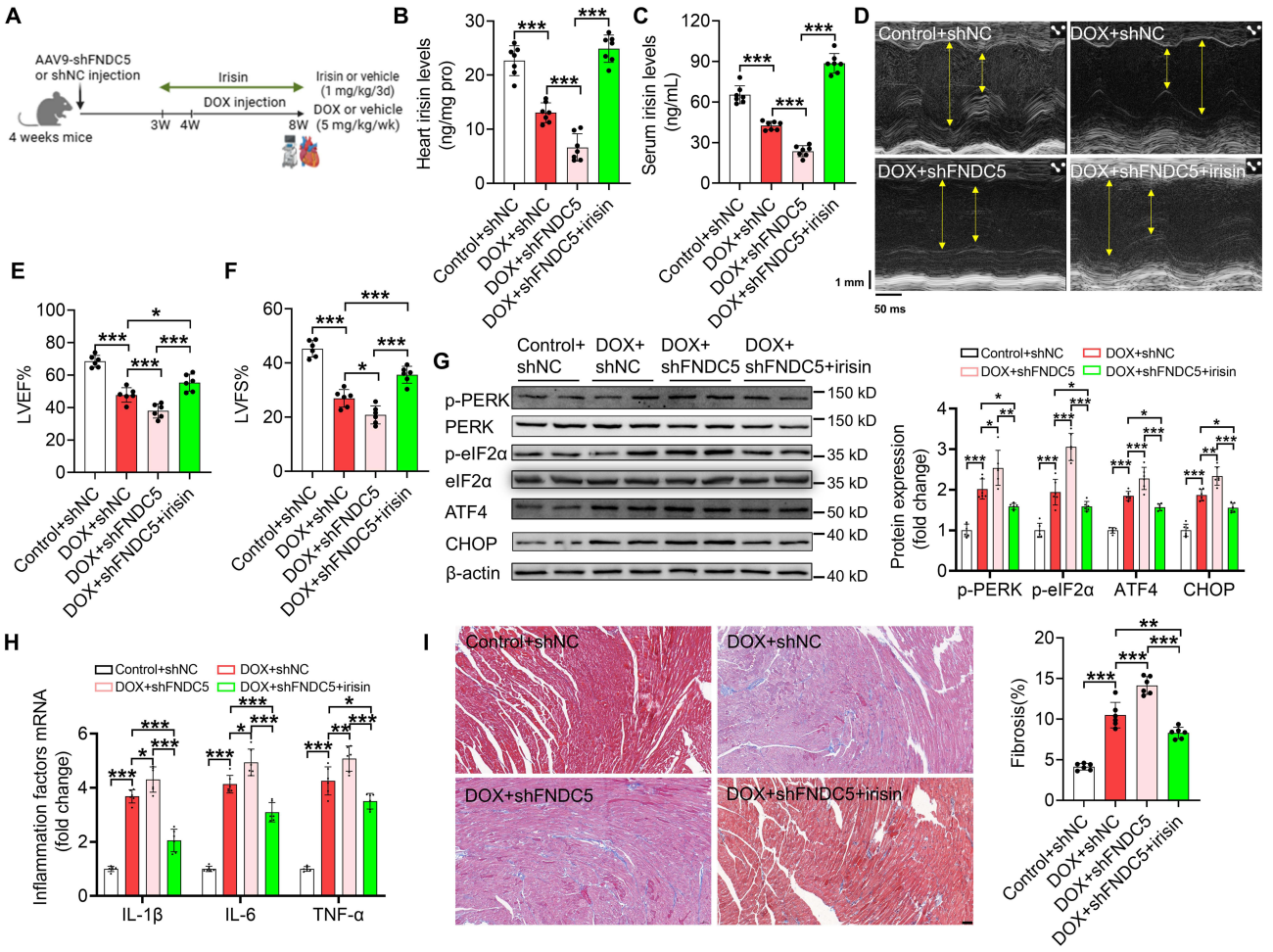

Figure 6 Irisin protect against DOX-induced myocardial injury through regulating the PERK-eIF2α-ATF4 pathway (n = 6 per group). (**A**) Schematic diagram depicting the experimental protocol with AAV9-shFNDC5 or AAV9-shNC injection in mice. (**B** and **C**) Serum irisin level (**B**) and heart irisin level (**C**). (**D**) Representative echocardiography images of heart in M-mode. (**E** and **F**) Quantification of LVEF% (**E**) and LVFS% (**F**). (**G**) Representative immunoblots and the quantification for protein expression of phospho- and total PERK, phospho-eIF2α, total-eIF2α, ATF4, and CHOP in heart tissues. β-actin as a loading control. (**H**) mRNA levels of IL-1β, IL-6, and TNF-α in heart tissues. (**I**) Representative heart sections stained with Masson trichrome (left) and quantification of the fibrosis area (right), scale bar=50 μm. Data are expressed as mean ± SD. * P < 0.05, **P < 0.01, and ***P < 0.001 was considered statistically significant.

activation of PERK-eIF2α-ATF4 pathway was enhanced in FNDC5-deficient mice, an effect that was partially reversed by irisin treatment (Figure 6G). Consequently, the exacerbated inflammatory and fibrotic responses in the heart were mitigated by irisin (Figure 6H and I).

In summary, the loss of irisin exacerbates the adverse cardiac effects induced by DOX, whereas irisin supplementation can ameliorate DOX-induced cardiotoxicity by inhibiting the PERK-eIF2α-ATF4 pathway activation.

Discussion

In this study, we demonstrated that irisin protects against DOX-induced cardiac injury by reducing cardiomyocyte apoptosis, oxidative stress, and inflammation. Irisin-treated mice exhibited improved cardiac function and reduced myocardial fibrosis to some extent. Moreover, we found that irisin effectively inhibited the activation of the PERK-eIF2α-ATF4 signaling pathway, suggesting its key role in the cardioprotective effects of irisin.

The FNDC5/irisin axis has been implicated in the pathology of cardiovascular diseases, including myocardial infarction and ischemia/reperfusion injury.[27,43–46] Clinical studies report lower circulating levels of irisin in patients with coronary artery disease compared to healthy controls.[47] Furthermore, irisin alleviates pressure overload-induced cardiac hypertrophy in mice.[29] Our results extend these findings by showing reduced FNDC5 expression and lower irisin

https://doi.org/10.2147/DDDT.S492691

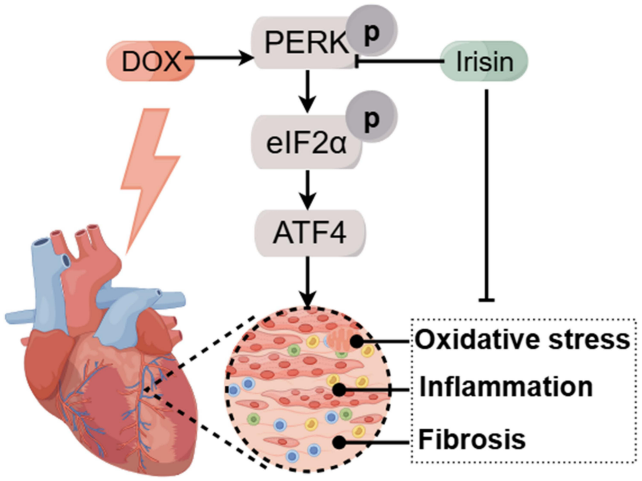

Figure 7 The role of irisin and the underlying mechanism in protecting against DOX-induced cardiotoxicity (Created by Figdraw (www.figdraw.com)).

levels in both cardiac tissue and serum following DOX treatment, suggesting that irisin may exert its protective effects in an autocrine or paracrine manner, particularly given the high expression of FNDC5 in the myocardium.[30]

Apoptosis is a critical contributor to the deterioration of cardiac function after DOX treatment.[46,48,49] Our study found that irisin treatment preserved heart contractility and reduced cardiomyocyte apoptosis after DOX treatment. Consistent with previous findings,[33,49,50] we observed that DOX increased the expression of pro-apoptotic factor Bax and decreased the anti-apoptotic factor Bcl-2. Irisin treatment improved the Bcl-2/Bax ratio, suggesting its role in promoting cell survival under DOX-induced stress. In addition, myocardial fibrosis and cardiac atrophy are key pathological characteristics of DOX-induced myocardial injury.[50] A substantial body of research has shown that DOX induces significant cardiac fibrosis, and we found that irisin treatment attenuated myocardial tissue and reduced fibrosis.[30,50,51] Recent studies suggest that DOX may trigger early endothelial-to-mesenchymal transition (EndMT), causing perivascular fibrosis in the heart. Unlike interstitial fibrosis, this form of fibrosis occurs around blood vessels, potentially leading to vascular stiffness and impaired cardiac function.[28] Differences in results may attribute to varying durations of DOX exposure and different assessment time points.

Irisin has been found to interact with SOD2, restoring its mitochondrial localization and ameliorating oxidative stress in the context of I/R injury.[43] Excessive ROS production, with a significant reduction in antioxidant enzyme activity, is associated with DOX cardiotoxicity.[52] Consistent with previous studies,[30,53] irisin reduced MDA and NADPH levels in the myocardium and increased the content of antioxidant enzymes GSH and SOD2 under DOX challenge. Additionally, irisin inhibited the production of pro-inflammatory cytokines such as IL-1β, IL-6, and TNF-α, which are elevated by DOX-induced oxidative stress, further supporting its anti-inflammatory effects. DOX-stimulated ROS production and inflammatory responses lead to lipid peroxidation and mitochondrial impairment. This study suggests that irisin improves mitochondrial structural damage and respiratory function caused by DOX. In vitro experiments further revealed that irisin inhibited overproduction of ROS and maintains mitochondrial function in DOX-treated H9c2 cells.

The role of the PERK-eIF2α-ATF4 pathway in DOX-induced cardiac injury remains debated. Disruption of PERK expression exacerbated pathological cardiac hypertrophy in the setting of pressure overload, as indicated by greater ventricular mass, decreased function, and increased ventricular dilation and fibrosis.[18] Conversely, activation of PERK-ATF4 has been observed in the progression of liver and aortic valve fibrosis.[54,55] Similarly, p-PERK and p-eIF2α expression significantly increased in angiotensin II (Ang II)-induced cardiac hypertrophy, participated in aggravated inflammation and fibrosis.[10] Overexpression of PERK or ATF4 has also been linked to cardiac atrophy and increased mortality in hearts subjected to pressure overload.[19] Our findings indicate that DOX activates the PERK-eIF2α-ATF4 pathway, a trend that is reduced by irisin treatment. Another study focusing on cardiac I/R injury also found that irisin alleviates I/R-induced ER stress upregulation.[27] To further explore this potential connection, we downregulated FNDC5 in the heart and found that these mice exhibited worsened cardiac function, aligning with previous studies.[28,35]

More importantly, heart-specific FNDC5-deficient mice exhibited worsened cardiac function and excessive activation of the PERK-eIF2α-ATF4 pathway following DOX stimulation. Although no differences of cardiac function were observed across all groups at the baseline, lower cardiac irisin levels in FNDC5-deficient mice might be a critical factor contributing to the exacerbated myocardial injury following DOX injection. Notably, supplementation with exogenous irisin rescued cardiac function, reduced cardiac fibrosis and inflammation, and inhibited the PERK-eIF2α-ATF4 signaling after FNDC5 knockdown. Wang et al found that deletion of eIF2α downregulates the expression of CHOP and protects against DOX-induced H9c2 cell death,[49] also suggesting that inhibition of the PERK-eIF2α-ATF pathway is beneficial for alleviating DOX-induced cardiotoxicity.

In conclusion, our study provides strong evidence that irisin exerts cardioprotective effects in DOX-induced cardiac injury by reducing oxidative stress, inflammation, and apoptosis, while improving mitochondrial function. Further, we demonstrated that irisin exerts its protective effects by inhibiting the PERK-eIF2α-ATF4 signaling, which is supported by using the heart-specific FNDC5 knockdown mice. Future studies will explore the involvement of other ER stress-related pathways, such as IRE1α and ATF6. Additionally, the direct interaction of irisin with the PERK protein are yet to be fully elucidated. One hypothesis is that irisin may exert its effects by directly binding to the PERK protein, which requires exploration through molecular docking and surface plasmon resonance (SPR) analysis. In our forthcoming research, we intend to undertake more in-depth investigations.

Conclusion

In conclusion, irisin effectively alleviates DOX-induced cardiac injury by reducing oxidative stress and inflammation, preserving mitochondrial function, and improving cardiac performance. It significantly decreases heart fibrosis and enhances ejection fraction. Furthermore, its protective effects were linked to the inhibition of the PERK-eIF2α-ATF4 pathway, as demonstrated in heart-specific FNDC5 knockdown mice, underscoring its potential in targeting DOX-induced cardiotoxicity (Figure 7).

Funding

This project was funded by the People's Hospital of Xinjiang Uygur Autonomous Region (No. 20210208).

Disclosure

The authors report no conflicts of interest in this work.

References

1. Wallace KB, Sardao VA, Oliveira PJ. Mitochondrial determinants of doxorubicin-induced cardiomyopathy. *Circ Res*. 2020;126(7):926–941. doi:10.1161/CIRCRESAHA.119.314681
2. Sciarretta S, Maejima Y, Zablocki D, Sadoshima J. The role of autophagy in the heart. *Annu Rev Physiol*. 2018;80:1–26. doi:10.1146/annurev-physiol-021317-121427
3. Wu L, Wang L, Du Y, Zhang Y, Ren J. Mitochondrial quality control mechanisms as therapeutic targets in doxorubicin-induced cardiotoxicity. *Trends Pharmacol Sci*. 2023;44(1):34–49. doi:10.1016/j.tips.2022.10.003
4. Christidi E, Brunham LR. Regulated cell death pathways in doxorubicin-induced cardiotoxicity. *Cell Death Dis*. 2021;12(4):339. doi:10.1038/s41419-021-03614-x
5. Shi S, Chen Y, Luo Z, Nie G, Dai Y. Role of oxidative stress and inflammation-related signaling pathways in doxorubicin-induced cardiomyopathy. *Cell Commun Signal*. 2023;21(1):61. doi:10.1186/s12964-023-01077-5
6. Tomczyk MM, Cheung KG, Xiang B, et al. Mitochondrial Sirtuin-3 (SIRT3) prevents doxorubicin-induced dilated cardiomyopathy by modulating protein acetylation and oxidative stress. *Circ Heart Fail*. 2022;15(5):e008547. doi:10.1161/CIRCHEARTFAILURE.121.008547
7. Picca A, Mankowski RT, Burman JL, et al. Mitochondrial quality control mechanisms as molecular targets in cardiac ageing. *Nat Rev Cardiol*. 2018;15(9):543–554. doi:10.1038/s41569-018-0059-z
8. Da Dalt L, Cabodevilla AG, Goldberg IJ, Norata GD. Cardiac lipid metabolism, mitochondrial function, and heart failure. *Cardiovasc Res*. 2023;119(10):1905–1914. doi:10.1093/cvr/cvad100
9. Zhao L, Qi Y, Xu L, et al. MicroRNA-140-5p aggravates doxorubicin-induced cardiotoxicity by promoting myocardial oxidative stress via targeting Nrf2 and Sirt2. *Redox Biol*. 2018;15:284–296. doi:10.1016/j.redox.2017.12.013
10. Zhang Y, Chen W, Wang Y. STING is an essential regulator of heart inflammation and fibrosis in mice with pathological cardiac hypertrophy via endoplasmic reticulum (ER) stress. *Biomed Pharmacother*. 2020;125:110022. doi:10.1016/j.biopha.2020.110022
11. Hsieh PL, Chu PM, Cheng HC, et al. Dapagliflozin Mitigates Doxorubicin-Caused Myocardium Damage by Regulating AKT-Mediated Oxidative Stress, Cardiac Remodeling, and Inflammation. *Int J mol Sci*. 2022;23(17):10146. doi:10.3390/ijms231710146

12. Belali OM, Ahmed MM, Mohany M, et al. LCZ696 protects against diabetic cardiomyopathy-induced myocardial inflammation, ER stress, and apoptosis through inhibiting AGEs/NF-κB and PERK/CHOP signaling pathways. *Int J mol Sci*. 2022;23(3):1288. doi:10.3390/ijms23031288
13. Palomer X, Román-Azcona MS, Pizarro-Delgado J, et al. SIRT3-mediated inhibition of FOS through histone H3 deacetylation prevents cardiac fibrosis and inflammation. *Signal Transduct Target Ther*. 2020;5(1):14. doi:10.1038/s41392-020-0114-1
14. Rashid HO, Yadav RK, Kim HR, Chae HJ. ER stress: autophagy induction, inhibition and selection. *Autophagy*. 2015;11(11):1956–1977. doi:10.1080/15548627.2015.1091141
15. Oakes SA, Papa FR. The role of endoplasmic reticulum stress in human pathology. *Annu Rev Pathol*. 2015;10:173–194. doi:10.1146/annurev-pathol-012513-104649
16. Jin JK, Blackwood EA, Azizi K, et al. ATF6 decreases myocardial ischemia/Reperfusion damage and links er stress and oxidative stress signaling pathways in the heart. *Circ Res*. 2017;120(5):862–875. doi:10.1161/CIRCRESAHA.116.310266
17. Kitakaze M, Tsukamoto O. What is the role of ER stress in the heart? Introduction and series overview. *Circ Res*. 2010;107(1):15–18. doi:10.1161/CIRCRESAHA.110.222919
18. Liu X, Kwak D, Lu Z, et al. Endoplasmic reticulum stress sensor protein kinase R-like endoplasmic reticulum kinase (PERK) protects against pressure overload-induced heart failure and lung remodeling. *Hypertension*. 2014;64(4):738–744. doi:10.1161/HYPERTENSIONAHA.114.03811
19. Vanhoutte D, Schips TG, Vo A, et al. Thbs1 induces lethal cardiac atrophy through PERK-ATF4 regulated autophagy. *Nat Commun*. 2021;12(1):3928. doi:10.1038/s41467-021-24215-4
20. Kim I, Xu W, Reed JC. Cell death and endoplasmic reticulum stress: disease relevance and therapeutic opportunities. *Nat Rev Drug Discov*. 2008;7(12):1013–1030. doi:10.1038/nrd2755
21. Ajoolabady A, Liu S, Klionsky DJ, et al. ER stress in obesity pathogenesis and management. *Trends Pharmacol Sci*. 2022;43(2):97–109. doi:10.1016/j.tips.2021.11.011
22. Ren J, Bi Y, Sowers JR, Hetz C, Zhang Y. Endoplasmic reticulum stress and unfolded protein response in cardiovascular diseases. *Nat Rev Cardiol*. 2021;18(7):499–521. doi:10.1038/s41569-021-00511-w
23. Maak S, Norheim F, Drevon CA, Erickson HP. Progress and Challenges in the Biology of FNDC5 and Irisin. *Endocr Rev*. 2021;42(4):436–456. doi:10.1210/endrev/bnab003
24. Kim H, Wrann CD, Jedrychowski M, et al. Irisin mediates effects on bone and fat via αV integrin receptors. *Cell*. 2018;175(7):1756–1768.e17. doi:10.1016/j.cell.2018.10.025
25. Perakakis N, Triantafyllou GA, Fernandez-Real JM, et al. Physiology and role of irisin in glucose homeostasis. *Nat Rev Endocrinol*. 2017;13(6):324–337. doi:10.1038/nrendo.2016.221
26. Ho MY, Wang CY. Role of Irisin in myocardial Infarction, heart failure, and cardiac hypertrophy. *Cells*. 2021;10(8):2103. doi:10.3390/cells10082103
27. Lu L, Ma J, Tang J, et al. Irisin attenuates myocardial ischemia/reperfusion-induced cardiac dysfunction by regulating ER-mitochondria interaction through a mitochondrial ubiquitin ligase-dependent mechanism. *Clin Transl Med*. 2020;10(5):e166. doi:10.1002/ctm2.166
28. Pan JA, Zhang H, Lin H, et al. Irisin ameliorates doxorubicin-induced cardiac perivascular fibrosis through inhibiting endothelial-to-mesenchymal transition by regulating ROS accumulation and autophagy disorder in endothelial cells. *Redox Biol*. 2021;46:102120. doi:10.1016/j.redox.2021.102120
29. Li RL, Wu SS, Wu Y, et al. Irisin alleviates pressure overload-induced cardiac hypertrophy by inducing protective autophagy via mTOR-independent activation of the AMPK-ULK1 pathway. *J mol Cell Cardiol*. 2018;121:242–255. doi:10.1016/j.yjmcc.2018.07.250
30. Zhang X, Hu C, Kong CY, et al. FNDC5 alleviates oxidative stress and cardiomyocyte apoptosis in doxorubicin-induced cardiotoxicity via activating AKT. *Cell Death Differ*. 2020;27(2):540–555. doi:10.1038/s41418-019-0372-z
31. Wen J, Zhang L, Liu H, et al. Salsolinol attenuates doxorubicin-induced chronic heart failure in rats and improves mitochondrial function in H9c2 cardiomyocytes. *Front Pharmacol*. 2019;10:1135. doi:10.3389/fphar.2019.01135
32. Wieckowski MR, Giorgi C, Lebiedzinska M, Duszynski J, Pinton P. Isolation of mitochondria-associated membranes and mitochondria from animal tissues and cells. *Nat Protoc*. 2009;4(11):1582–1590. doi:10.1038/nprot.2009.151
33. Li H, Zhang M, Wang Y, et al. Daidzein alleviates doxorubicin-induced heart failure via the SIRT3/FOXO3a signaling pathway. *Food Funct*. 2022;13(18):9576–9588. doi:10.1039/d2fo00772j
34. Sun Z, Lu W, Lin N, et al. Dihydromyricetin alleviates doxorubicin-induced cardiotoxicity by inhibiting NLRP3 inflammasome through activation of SIRT1. *Biochem Pharmacol*. 2020;175:113888. doi:10.1016/j.bcp.2020.113888
35. Ren W, Xu Z, Pan S, et al. Irisin and ALCAT1 mediated aerobic exercise-alleviated oxidative stress and apoptosis in skeletal muscle of mice with myocardial infarction. *Free Radic Biol Med*. 2022;193(Pt 2):526–537. doi:10.1016/j.freeradbiomed.2022.10.321
36. Quagliariello V, De laurentiis M, Rea D, et al. The SGLT-2 inhibitor empagliflozin improves myocardial strain, reduces cardiac fibrosis and pro-inflammatory cytokines in non-diabetic mice treated with doxorubicin. *Cardiovasc Diabetol*. 2021;20(1):150. doi:10.1186/s12933-021-01346-y
37. Abderrazak A, Syrovets T, Couchie D, et al. NLRP3 inflammasome: from a danger signal sensor to a regulatory node of oxidative stress and inflammatory diseases. *Redox Biol*. 2015;4:296–307. doi:10.1016/j.redox.2015.01.008
38. Zhang S, Liu X, Bawa-Khalfe T, et al. Identification of the molecular basis of doxorubicin-induced cardiotoxicity. *Nat Med*. 2012;18(11):1639–1642. doi:10.1038/nm.2919
39. Carvalho FS, Burgeiro A, Garcia R, et al. Doxorubicin-induced cardiotoxicity: from bioenergetic failure and cell death to cardiomyopathy. *Med Res Rev*. 2014;34(1):106–135. doi:10.1002/med.21280
40. Octavia Y, Tocchetti CG, Gabrielson KL, et al. Doxorubicin-induced cardiomyopathy: from molecular mechanisms to therapeutic strategies. *J mol Cell Cardiol*. 2012;52(6):1213–1225. doi:10.1016/j.yjmcc.2012.03.006
41. Wang Y, Jasper H, Toan S, et al. Mitophagy coordinates the mitochondrial unfolded protein response to attenuate inflammation-mediated myocardial injury. *Redox Biol*. 2021;45:102049. doi:10.1016/j.redox.2021.102049
42. Liu J, Huang Y, Liu Y, Chen Y. Irisin Enhances Doxorubicin-Induced Cell Apoptosis in Pancreatic Cancer by Inhibiting the PI3K/AKT/NF-κB Pathway. *Med Sci Monit*. 2019;25:6085–6096. doi:10.12659/msm.917625
43. Wang Z, Chen K, Han Y, et al. Irisin protects heart against ischemia-reperfusion injury through a SOD2-dependent mitochondria mechanism. *J Cardiovasc Pharmacol*. 2018;72(6):259–269. doi:10.1097/fjc.0000000000000608

44. Jin L, Piao Z. Irisin protects against cardiac injury by inhibiting NLRP3 inflammasome-mediated pyroptosis during remodeling after infarction. *Int Immunopharmacol*. 2024;130:111714. doi:10.1016/j.intimp.2024.111714
45. Kuloglu T, Aydin S, Eren MN, et al. Irisin: a potentially candidate marker for myocardial infarction. *Peptides*. 2014;55:85–91. doi:10.1016/j.peptides.2014.02.008
46. Wu X, Wang L, Wang K, et al. ADAR2 increases in exercised heart and protects against myocardial infarction and doxorubicin-induced cardiotoxicity. *Mol Ther*. 2022;30(1):400–414. doi:10.1016/j.ymthe.2021.07.004
47. Anastasilakis AD, Koulaxis D, Kefala N, et al. Circulating irisin levels are lower in patients with either stable coronary artery disease (CAD) or myocardial infarction (MI) versus healthy controls, whereas follistatin and activin A levels are higher and can discriminate MI from CAD with similar to CK-MB accuracy. *Metabolism*. 2017;73:1–8. doi:10.1016/j.metabol.2017.05.002
48. Arola OJ, Saraste A, Pulkki K, et al. Acute doxorubicin cardiotoxicity involves cardiomyocyte apoptosis. *Cancer Res*. 2000;60(7):1789–1792.
49. Wang Y, Lei T, Yuan J, et al. GCN2 deficiency ameliorates doxorubicin-induced cardiotoxicity by decreasing cardiomyocyte apoptosis and myocardial oxidative stress. *Redox Biol*. 2018;17:25–34. doi:10.1016/j.redox.2018.04.009
50. Ding M, Shi R, Fu F, et al. Paeonol protects against doxorubicin-induced cardiotoxicity by promoting Mfn2-mediated mitochondrial fusion through activating the PKCε-Stat3 pathway. *J Adv Res*. 2023;47:151–162. doi:10.1016/j.jare.2022.07.002
51. Liu X, Li D, Pi W, et al. LCZ696 protects against doxorubicin-induced cardiotoxicity by inhibiting ferroptosis via AKT/SIRT3/SOD2 signaling pathway activation. *Int Immunopharmacol*. 2022;113(Pt A):109379. doi:10.1016/j.intimp.2022.109379
52. Stěrba M, Popelová O, Vávrová A, et al. Oxidative stress, redox signaling, and metal chelation in anthracycline cardiotoxicity and pharmacological cardioprotection. *Antioxid Redox Signal*. 2013;18(8):899–929. doi:10.1089/ars.2012.4795
53. Zhuo C, Xin J, Huang W, et al. Irisin protects against doxorubicin-induced cardiotoxicity by improving AMPK-Nrf2 dependent mitochondrial fusion and strengthening endogenous anti-oxidant defense mechanisms. *Toxicology*. 2023;494:153597. doi:10.1016/j.tox.2023.153597
54. Xiong Z, Li J, Huang R, et al. The gut microbe-derived metabolite trimethylamine-N-oxide induces aortic valve fibrosis via PERK/ATF-4 and IRE-1α/XBP-1s signaling in vitro and in vivo. *Atherosclerosis*. 2024;391:117431. doi:10.1016/j.atherosclerosis.2023.117431
55. Koo JH, Lee HJ, Kim W, Kim SG. Endoplasmic reticulum stress in hepatic stellate cells promotes liver fibrosis via PERK-mediated degradation of HNRNPA1 and up-regulation of SMAD2. *Gastroenterology*. 2016;150(1):181–193.e8. doi:10.1053/j.gastro.2015.09.039